

TLR7 agonist administration to SIV-infected macaques receiving early initiated cART does not induce plasma viremia

Gregory Q. Del Prete, ... , Romas Geleziunas, Jeffrey D. Lifson

JCI Insight. 2019;4(11):e127717. <https://doi.org/10.1172/jci.insight.127717>.

Research Article

AIDS/HIV

Reduction/elimination of HIV-1 reservoirs that persist despite combination antiretroviral therapy (cART) will likely require induction of viral expression by residual infected cells and enhanced clearance of these cells. TLR7 agonists have potential to mediate these activities. We evaluated immunologic and virologic effects of repeated doses of the TLR7 agonist GS-9620 in SIV-infected rhesus macaques receiving cART, which was initiated at 13 days after infection and was continued for 75 weeks prior to GS-9620 administration. During cART, GS-9620 induced transient upregulation of IFN-stimulated genes in blood and tissues, increases in plasma cytokines, and changes in immune cell population activation and phenotypes but did not result in measurable increases in plasma viremia or viral RNA-to-viral DNA ratio in PBMCs or tissues nor decreases in viral DNA in PBMC or tissues. SIV-specific CD8⁺ T cell responses, negligible prior to GS-9620 treatment, were not measurably boosted by treatment; a second course of GS-9620 administration overlapping with later cART discontinuation was associated with increased CD8⁺ T cell responses during viral recrudescence. These results confirm and extend evidence for GS-9620-mediated enhancement of antiviral immune responses in SIV-infected macaques but suggest that GS-9620-mediated viral induction may depend critically on the timing of initiation and duration of cART and resulting characteristics of viral reservoirs.

Find the latest version:

<https://jci.me/127717/pdf>



TLR7 agonist administration to SIV-infected macaques receiving early initiated cART does not induce plasma viremia

Gregory Q. Del Prete,¹ W. Gregory Alvord,² Yuan Li,¹ Claire Deleage,¹ Mukta Nag,¹ Kelli Oswald,¹ James A. Thomas,¹ Cathi Pyle,¹ William J. Bosche,¹ Vicky Coalter,¹ Adam Wiles,¹ Rodney Wiles,¹ Brian Berkemeier,¹ Michael Hull,¹ Elizabeth Chipriano,¹ Lorna Silipino,¹ Randy Fast,¹ Jacob Kiser,¹ Rebecca Kiser,¹ Tyler Malys,² Joshua Kramer,³ Matthew W. Breed,³ Charles M. Trubey,¹ Jacob D. Estes,¹ Tiffany L. Barnes,⁴ Joseph Hesselgesser,⁴ Romas Geleziunas,⁴ and Jeffrey D. Lifson¹

¹AIDS and Cancer Virus Program, ²DMS Applied Information & Management Sciences, and ³Laboratory Animal Sciences Program, Frederick National Laboratory for Cancer Research, Frederick, Maryland, USA. ⁴Gilead Sciences, Foster City, California, USA.

Reduction/elimination of HIV-1 reservoirs that persist despite combination antiretroviral therapy (cART) will likely require induction of viral expression by residual infected cells and enhanced clearance of these cells. TLR7 agonists have potential to mediate these activities. We evaluated immunologic and virologic effects of repeated doses of the TLR7 agonist GS-9620 in SIV-infected rhesus macaques receiving cART, which was initiated at 13 days after infection and was continued for 75 weeks prior to GS-9620 administration. During cART, GS-9620 induced transient upregulation of IFN-stimulated genes in blood and tissues, increases in plasma cytokines, and changes in immune cell population activation and phenotypes but did not result in measurable increases in plasma viremia or viral RNA-to-viral DNA ratio in PBMCs or tissues nor decreases in viral DNA in PBMC or tissues. SIV-specific CD8⁺ T cell responses, negligible prior to GS-9620 treatment, were not measurably boosted by treatment; a second course of GS-9620 administration overlapping with later cART discontinuation was associated with increased CD8⁺ T cell responses during viral recrudescence. These results confirm and extend evidence for GS-9620-mediated enhancement of antiviral immune responses in SIV-infected macaques but suggest that GS-9620-mediated viral induction may depend critically on the timing of initiation and duration of cART and resulting characteristics of viral reservoirs.

Introduction

Although combination antiretroviral therapy (cART) can effectively suppress ongoing HIV-1 replication for many years, currently available agents can only inhibit new rounds of infection and cannot directly eliminate already infected cells. Cellular sources of replication-competent HIV-1, i.e., “viral reservoirs,” therefore persist despite long-term cART. These long-lived sources of replication-competent virus can initiate viral recrudescence and the reestablishment of disseminated, ongoing viral replication if cART is discontinued (1, 2). Thus, although modern cART is highly effective (3), lifelong treatment with antiretroviral drugs is required for the vast majority of infected people. Such lifelong treatment comes at considerable financial cost, and concerns remain over global access to treatment and compliance for many decades of daily drug administration (4, 5). In addition, effectively treated individuals maintain elevated levels of immune activation and higher rates of non-AIDS morbidities than uninfected people (6), and some of these issues may be due to the continued presence of virally infected cells in treated people (7–10). For these reasons, there is a substantial scientific effort to identify definitive treatment approaches for HIV infection that would obviate the need for lifelong cART.

CD4⁺ T cells harboring replication-competent virus can be isolated from infected individuals after decades of suppressive therapy and are a primary component of the viral reservoir (11–14). Persistence of these cells can be largely attributed to two nonmutually exclusive mechanisms: prolonged survival of resting, latently infected cells (12–15), and the cell division and clonal expansion of cells with integrated

Conflict of interest: TLB, JH, and RG are employees of Gilead Sciences and may own Gilead Sciences stock and/or stock options.

Copyright: © 2019, American Society for Clinical Investigation.

Submitted: January 31, 2019

Accepted: April 19, 2019

Published: June 6, 2019.

Reference information: *JCI Insight*. 2019;4(11):e127717. <https://doi.org/10.1172/jci.insight.127717>.

viral genomes (16–20). Ongoing viral replication, particularly within tissues in which cART penetration may be suboptimal, has also been proposed as a potential mechanism for viral persistence (7, 9, 21–24), but current data do not support this mechanism as a substantive contributor of viral persistence (8, 25–34). A stable reservoir of latently infected CD4⁺ T cells is likely the chief obstacle to HIV-1 remission or viral eradication. This pool of latently infected cells poses a challenging therapeutic target for interventions designed to eliminate it because it is composed of cells that are essentially indistinguishable from uninfected cells.

Efforts to reduce or eliminate these residual infected CD4⁺ T cells therefore generally involve two broad goals: (a) stimulate the induced production of viral gene products from residual infected cells (i.e., latency reversal) to allow for their targeting by immune-mediated or other means and (b) engender or enhance antiviral immune responses or employ other targeting approaches with the capacity to eliminate targeted cells. To date, most in vivo studies of potential viral cure/eradication modalities have involved evaluations of agents proposed to only achieve one of these two goals, with the expectation that a combination of promising approaches will then be required to identify a successful reservoir reduction/elimination strategy. For this reason, single agents with the potential to both reactivate virus and enhance the killing of cells expressing viral gene products are highly sought after. Indeed, as some latency-reversing agents have been suggested to have undesirable, potentially immunosuppressive properties (35–38), a potent latency-reversing agent that instead enhances antiviral immune responses would be a highly valuable component of an HIV cure strategy.

A recent report by Lim and coworkers showed promising results for both the potential viral reactivation activity and immune-boosting capacity of TLR7 agonists in SIV-infected macaques (39). The small-molecule TLR7 agonists GS-9620 (Vesatolimod) and GS-986 (Vesatolimod analog) were orally administered once every 2 weeks to SIVmac251-infected rhesus macaques that received cART starting 65 days after infection (dpi) and given for approximately 400 days prior to the first dose of TLR7 agonist. The authors reported activation of innate and adaptive immune cell populations and transient increases in plasma SIV RNA (i.e., “blips”) after TLR7 agonist administrations, following an induction phase of several initial TLR7 agonist doses without any apparent plasma virus blips. This finding, coupled with apparent reductions in viral DNA (vDNA) levels in peripheral blood mononuclear cells (PBMCs) and tissues and reductions in the amount of viral RNA (vRNA) produced by stimulated cells in ex vivo cell cultures following multiple doses of TLR7 agonist, was suggestive of drug activity that both induced the reactivation (or increased activation) of virus expression by residual infected cells and enhanced the clearance of these cells, perhaps through boosting of immune responses. Most intriguingly, in 2 of 9 animals released from cART following multiple TLR7 agonist doses, there was no measurable virologic rebound during follow-up, which included the experimental antibody-mediated depletion of CD8⁺ cells and the adoptive transfer of cells from these 2 animals into naive recipients, which also remained aviremic.

Given these findings, which were broadly consistent with prior in vitro studies indicating modest virus induction activity for GS-9620 (40), and remaining questions about the in vivo mechanism of action for TLR7 agonists, particularly in tissues, we evaluated GS-9620 treatment in a cohort of SIV-infected rhesus macaques that were started on cART at approximately peak viremia (day 13 after infection) and maintained on suppressive therapy for a longer duration prior to the initiation of GS-9620 dosing. We reasoned that earlier and longer cART administration prior to GS-9620 dosing, would establish smaller viral reservoirs in our animals and preserve a more intact immune system, thereby increasing the likelihood of viral remission, similar to that seen in the Lim et al. study (39).

Results

Study design and virologic suppression on cART. Six Indian-origin rhesus macaques were intravenously infected with SIVmac239X (41) and treated with an effective cART regimen (42) starting at 13 dpi (i.e., approximately at peak viremia; Figure 1). Plasma viral loads (pVLs) declined from peak levels of 1.1×10^7 to 8.7×10^7 vRNA copies/ml prior to cART initiation to <30 vRNA copies/ml within 7–20 weeks of cART initiation (Figure 2). Starting at 48 weeks after treatment initiation, a more sensitive pVL assay with a quantification limit of 15 vRNA copies/ml was employed for the remainder of the study. Between 20 and 73 weeks on cART, only 5 of 161 plasma samples analyzed across all animals had detectable vRNA levels above assay threshold quantification limits (i.e., >30 vRNA copies/ml between 20 and 46 weeks or >15 vRNA copies/ml between 48 and 75 weeks on cART) (Figure 2). After approximately 1.5 years (75 weeks) of cART, at which point the animals had been well suppressed for 55–68 weeks, the animals were divided

into GS-9620 ($n = 4$) and vehicle control ($n = 2$) treatment groups. For the first course of GS-9620 treatments, consisting of 12 doses in total (cycle 1, doses 1–12; designated as 1.1 to 1.12) administered concomitantly with cART, each animal received 2 doses of GS-9620 at 0.15 mg/kg (doses 1.1 to 1.2) followed by 10 doses at 0.5 mg/kg (doses 1.3 to 1.12) (Figure 1). GS-9620 doses were administered once every 2 weeks, except for a 3-week gap between doses 1.9 and 1.10, due to the collection of biopsy specimens following dose 1.9. Animals were then maintained on cART without GS-9620 administrations for a 40- to 41-week rest period, followed by a second course of GS-9620 dosing, consisting of another 5 doses (cycle 2, doses 1–5; designated as 2.1 to 2.5) administered at 0.15 mg/kg and overlapping with cART discontinuation. The final cART administration was concomitant with GS-9620 dose 2.3, with doses 2.1 and 2.2 occurring on cART and doses 2.4 and 2.5 occurring after cART cessation. Vehicle control animals received an equivalent volume of drug vehicle on the same schedule as GS-9620 treatments and were otherwise treated the same as the GS-9620 group. In total, all 6 animals received suppressive cART for 144 weeks or approximately 2.75 years. The cART regimen was well tolerated in all animals throughout the treatment period, with no serum chemistry abnormalities noted (data not shown).

GS-9620 activity in vivo. TLR7 stimulation results in type I IFN production by plasmacytoid dendritic cells (43). Effective engagement of TLR7 by GS-9620 has accordingly been shown to result in the upregulation of specific IFN-stimulated genes (ISGs) (40, 44–47). Therefore, to assess the *in vivo* pharmacodynamic activity of GS-9620, we utilized an ISG mRNA expression array to compare responses in PBMCs collected from GS-9620-treated and vehicle control animals immediately prior to and at 24 hours after administration of the first 8 doses of GS-9620. At the 24-hour time point, multiple ISGs were substantially upregulated in the GS-9620-treated animals compared with vehicle control animals, including a significantly greater upregulation of ISG15, IFI27, IFIT3, CXCL10, MX1, IRF7, OAS2, and MX2 (Figure 3 and Supplemental Figure 1; supplemental material available online with this article; <https://doi.org/10.1172/jci.insight.127717DS1>). Among these genes, the greatest mean magnitude of upregulated expression was measured for ISG15 (112-fold), followed by IFI27 (63-fold), IFIT3 (37-fold), CXCL10 (32-fold), MX1 (20-fold), IRF7 (18-fold), OAS2 (17-fold), and MX2 (16-fold; Figure 3).

We also measured significantly higher levels of several cytokines in the plasma of GS-9620-treated animals compared with controls at 24 hours after GS-9620 administration. Plasma cytokine levels were measured immediately prior to and at 24 hours after GS-9620 doses 1.1 to 1.7 and doses 1.10 to 1.12 (Figure 4). Plasma IFN- α , IL-1RA, and CXCL11 (also known as I-TAC) levels were all significantly higher in the GS-9620-treated animals compared with the control animals across the 24-hour time points (Figure 4). There was also a trend toward a small (~3-fold) increase in plasma TNF- α levels across the 24-hour time points in the GS-9620-treated animals, but this increase in TNF- α levels was not significantly different than that in the control animals, likely due to a consistent lack of a measurable TNF- α response in 1 of the GS-9620-treated animals (Supplemental Figure 2) Consistent with these induced increases being transient and returning to baseline shortly after each GS-9620 dose, there were no differences between the treatment groups across the 10 before dose time points.

Because the majority of viral reservoirs likely reside in tissues (48), we also evaluated the pharmacodynamic activity of orally administered GS-9620 in lymph nodes (LNs), upper gastrointestinal (GI) tissue, and rectal tissue (Figure 5). Immunohistochemical staining for ISG15 protein was performed on tissue specimens collected prior to the first dose of GS-9620 and at 24 hours and 48 hours following dose 1.9. ISG15 staining was indistinguishable between the GS-9620 and control groups prior to GS-9620 dosing; however, ISG15 levels transiently increased in GS-9620 animals but not control animals at 24 hours after GS-9620 dose before declining to near-baseline levels by 48 hours after dose, consistent with drug activity in key sites harboring viral reservoirs (Figure 5). In LNs, ISG15 was elevated not only in the T cell zone, but also in the LN follicles (Figure 5A), a tissue site that has been proposed as a key sanctuary site for viral reservoir persistence (49–55).

Immunologic responsiveness to GS-9620 administrations. We longitudinally monitored multiple immune cell subsets in blood by flow cytometry prior to and at 24 and 48 hours following each of the 12 doses constituting the first course of GS-9620 (doses 1.1 to 1.12). Overall, the most pronounced responses to GS-9620 were measured at 24 hours after each dose, with many parameters returning to baseline or near-baseline levels by 48 hours. CD8⁺ T cell counts in blood transiently decreased by an average of 2.9-fold (mean decline of 648 CD8⁺ T cells/ μ l) and were significantly lower in GS-9620-treated animals than in control animals at 24 hours after dose (Figure 6A). By contrast, there was no difference in CD8⁺ T cell

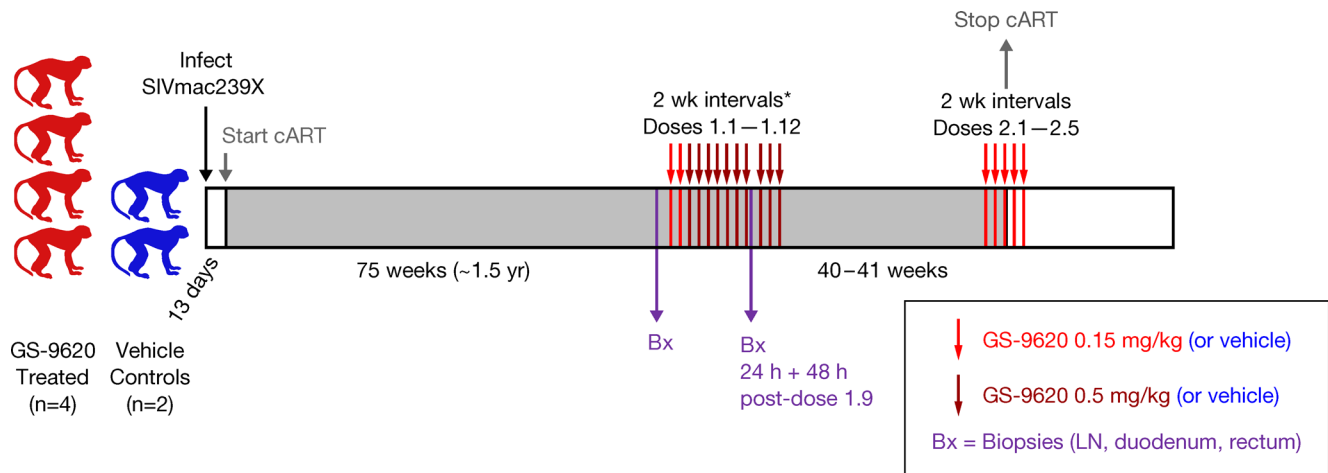


Figure 1. Study schema. Study design, including timing of cART initiation (gray downward arrow), tissue sampling (Bx, purple arrows), GS-9620 administrations (red arrows), and cART cessation (gray upward arrow), is shown. GS-9620 dose for each administration is indicated by arrow color. All 6 study animals were treated as shown, with the exception that the 2 vehicle control animals received only drug vehicle instead of GS-9620 at each of the GS-9620 treatment time points. The asterisk indicates that doses 1.1 through 1.12 were administered at 2-week intervals, except for dose 1.10, which was administered 3 weeks after dose 1.9.

count between the groups across the pretreatment and 48-hour time points (Figure 6A), and the frequency of CD8⁺ T cells expressing the lymphoid homing markers CCR7 and CXCR5 was elevated at 24 hours after dose (Supplemental Figure 3), suggesting that the transient decrease in CD8⁺ T cell count reflected redistribution of the cells from the blood, rather than their loss. CD8⁺ T cell activation was also modulated by GS-9620 treatment. CD38 expression (mean percentage of CD38⁺ increasing from 71% to 90%) was significantly elevated in the GS-9620-treated animals compared with the vehicle control animals across the 24-hour and 48-hour time points (Figure 6A). Coexpression of CD38 and HLA-DR on CD8⁺ T cells was also significantly upregulated across the 24-hour and 48-hour time points in GS-9620-treated animals compared with controls (Supplemental Figure 4). Although there were no significant differences in CD4⁺ T cell counts between the treated and control groups, there was a trend toward elevated CD38 positivity in the GS-9620-treated animals' CD4⁺ T cells at 24 hours after dose ($P = 0.073$; Figure 6B).

Several innate immune cell populations also responded to GS-9620 treatment. Similar to CD8⁺ T cells, total NK cell counts were significantly lower in GS-9620-treated animals than in control animals across the 24-hour time points but not before treatment or at 48 hours after dose (Figure 6C), with an approximately 10-fold average decline (mean decline of 332 NK cells/ μ l) in NK cell counts at 24 hours. Similar to CD8⁺ T cell counts, the brief, transient nature of this dramatic decline in blood NK cell count, coupled with an elevated frequency of CCR7- and CXCR5-expressing NK cells at 24 hours after GS-9620 administration (Supplemental Figure 3B), was suggestive of NK cell redistribution into tissues rather than cell loss. HLA-DR surface expression, a marker of NK cell activation, was also significantly elevated at 24 hours, though this was only observed on CD56⁺CD16⁻ but not CD56⁺CD16⁺ NK cells (mean percentage of HLA-DR⁺ increasing from 3.2% to 7.5%; Figure 6C and Supplemental Figure 5). The most striking effects of GS-9620 treatment were observed in circulating monocyte/macrophage (M/M) populations. Although CD56 is viewed as an NK cell marker in humans, in healthy macaques, the vast majority of M/M in the blood typically express CD56 (56). Although there were no differences in total M/M counts between the treatment groups across any of the measured time points (Figure 6D), there was a dramatic inversion in the percentage of M/M cells expressing CD56 and those expressing CD16 following GS-9620 administration (Figure 6D). When compared with the corresponding pretreatment time points in GS-9620-treated animals, across the 24-hour time points, the percentage of M/M that were CD56⁺CD16⁻ declined substantially (mean percentage of CD56⁺CD16⁻ decreasing from 81% to 18%) (Figure 6D), while the percentage of M/M that were CD56⁺CD16⁺ and CD56⁻CD16⁺ increased substantially (mean percentage of CD56⁺CD16⁺ increasing from 1.9% to 35%; mean percentage of CD56⁻CD16⁺ increasing from 5.5% to 19%), respectively (Figure 6D). These changes were clearly drug related, as the percentage of the CD56⁺CD16⁻ M/M population was significantly lower while the inverse percentage of the CD56⁻CD16⁺ M/M population was significantly higher in the GS-9620-treated animals compared with the control animals across the 24-hour time

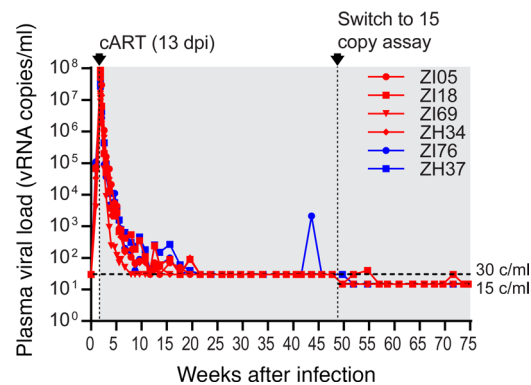


Figure 2. Plasma viral loads prior to GS-9620 administration. Longitudinal SIV RNA quantification in plasma is shown for the first 75 weeks of the study, which includes time points from before cART through the first 73 weeks on cART (plot region with a gray background). Red plots are for animals later treated with GS-9620; blue plots are for vehicle control animals. The plasma viral load assay used was switched from one with a 30 vRNA copy/ml threshold sensitivity to one with a 15 vRNA copy/ml threshold sensitivity at the indicated time point. Plasma viral load data for these 6 animals through the first 42 weeks have been reported previously (42).

points, with no differences between the groups at the pretreatment time points. Although the magnitude of the differences between the treatment groups were less pronounced at 48 hours after dose, the percentage of M/M that were CD56⁺CD16⁺ were still significantly elevated in the GS-9620 treatment group at this time point. The percentage of M/M that were CD56⁺CD16⁻ was also markedly lower at 48 hours in the treated animals compared with the control animals. Due to the heteroscedasticity introduced by the extreme sustained responses measured in treated animal ZH34, this latter result was not significant. If this animal, with the most pronounced effect at 48 hours, is omitted from the analysis, the difference between the GS-9620 and control groups is highly significant ($P = 0.005$). Taken together, these findings show clear responses to GS-9620 dosing by multiple immune cell populations in the treated animals and further confirm that biologically active doses of the drug were administered.

Virologic activity of GS-9620. SIV RNA was quantified in plasma samples collected immediately prior to each GS-9620 dose and then at 24 hours, 48 hours, and 7 days following each of the 12 doses of GS-9620 cycle 1 (Figure 7A). There were no increases in pVL measurements in association with GS-9620 dosing. SIV RNA levels were maintained below 15 vRNA copies/ml throughout the 12 doses of GS-9620 for all 6 animals, except for a single blip in 1 GS-9620–treated animal and 2 blips in 1 vehicle control animal. In GS-9620–treated animal ZI18, we measured 30 vRNA copies/ml plasma at 48 hours after dose 1.7, the fifth dose administered at 0.5 mg/kg. In control animal ZH37, we measured 30 vRNA copies/ml at 48 hours after vehicle administration 1.1 and 40 vRNA copies/ml at 48 hours after vehicle administration 1.11. In both cases, the measured increase in pVL was transient, with levels returning to <15 copies/ml by the next assayed time point; all these blips were lower than the nominal 50-copy/ml assay sensitivity cutoff based on the assay used in the Lim et al. study (39). We note that the single GS-9620 animal that exhibited a plasma viremia blip following dose 1.7 had a similar blip of 30 vRNA copies/ml 5 weeks prior to the first dose of GS-9620 (i.e., 87 weeks after cART initiation).

Because the animals in this study started on suppressive cART relatively early after infection (13 dpi) and were then maintained on cART for nearly 1.5 years prior to GS-9620 dosing, it was possible that the inducible viral reservoir was too small to produce enough virus to result in a measurable change in pVLs, even if reactivated. We therefore also quantified cell- and tissue-associated vRNA and vDNA, both extracted from the same specimens, and calculated the ratio of these 2 values as a measure of viral transcriptional activation. We did not observe any consistent increases in CD4-normalized vRNA levels (Supplemental Figure 6) or viral transcriptional ratios (Figure 7B) at 24 or 48 hours after dose in the PBMCs of GS-9620–treated animals, as might be expected if robust viral reactivation had occurred. For the GS-9620–treated animals, the mean transcriptional ratios (vRNA copies/vDNA copy) at pretreatment, 24-hour, and 48-hour time points were 0.58, 0.68, and 0.46, respectively, while for the control animals the pretreatment, 24-hour, and 48-hour mean transcriptional ratios were 0.35, 0.3, and 0.32, respectively. Similarly, in LN, upper GI, and rectal tissue, there were no apparent GS-9620–associated

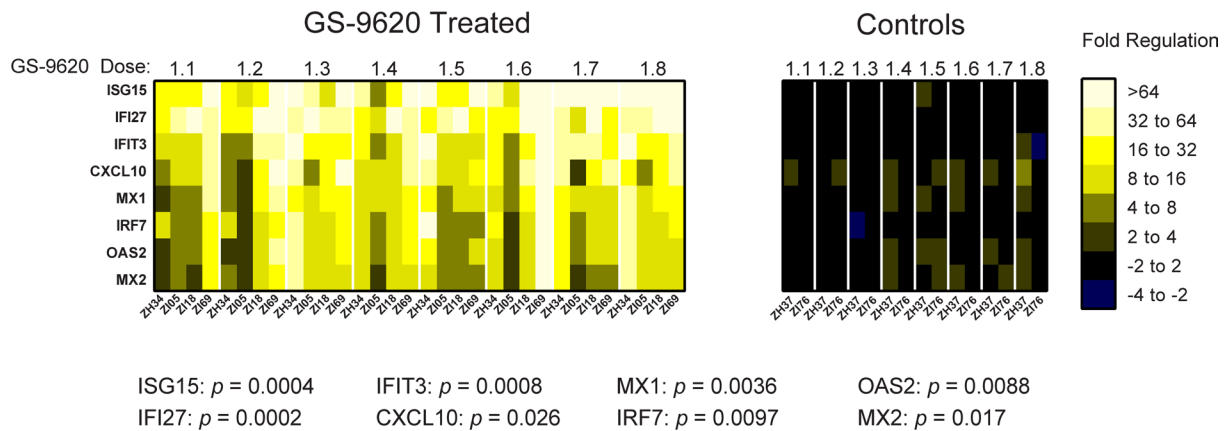


Figure 3. Upregulation of IFN-stimulated gene expression following GS-9620 administration. The RNA expression level in PBMCs of each of the indicated IFN-stimulated genes (ISGs) was determined immediately prior to and at 24 hours following each of the first 8 doses of GS-9620 (doses 1.1 to 1.8) for all 6 study animals. For each animal, dose, and gene, the fold change in expression in PBMCs collected at the 24-hour time point compared with PBMCs collected prior to the corresponding dose is shown, with upregulation expressed as positive values and downregulation expressed as negative values. Shown are the fold-change values for the 8 most greatly upregulated genes following GS-9620 administration.

differences in the transcriptional ratios calculated for samples collected prior to GS-9620 dosing and at 24 hours and 48 hours after dose 1.9 (Figure 7C).

Although our virologic measurements did not suggest viral reactivation in association with GS-9620 administration, we compared vDNA levels in PBMCs and in tissues to determine if vDNA levels declined after multiple doses of GS-9620. Immediately prior to GS-9620 administration, vDNA levels in PBMCs ranged from approximately 70–180 copies per 10^5 cell equivalents (Figure 8). There were no consistent changes in vDNA levels across animals after all 12 doses of GS-9620. Two GS-9620-treated animals demonstrated a modest decline in measured vDNA levels (lower by less than 3-fold; 55%–62% lower) while the measured vDNA levels in the other two treated animals were higher by 1.7- to 1.9-fold (70%–90% higher) (Figure 8). In the control animals, vDNA levels in PBMCs declined by 1.2- to 1.8-fold (14%–43% lower) after 12 vehicle doses (Figure 8). We similarly did not measure any consistent reductions in vDNA levels in LNs or upper or lower GI tissues following multiple GS-9620 doses. LN, upper GI, and lower GI tissue biopsy specimens were collected from each animal prior to GS-9620 dose 1.1 and following GS-9620 dose 1.9 (i.e., 18 weeks after dose 1.1 pretreatment samples were collected). Because heterogeneous tissue specimens collected via biopsy can be subject to sampling differences, we determined vDNA levels in tissues collected at 2 time points separated by only 24 hours, a time period during which total vDNA levels would not be expected to change substantially. For each of the 3 tissue types collected, we did not measure any declines or increases in vDNA levels that were consistent or maintained between 24 hours and 48 hours after dose 1.9 for either treatment group (Figure 8), consistent with the view that any measured differences between the dose 1.1 pretreatment samples and samples collected after dose 1.9 are likely driven by differences in sampling relatively small amounts of heterogeneous tissues.

Immune response boosting by TLR7 agonist dosing. Borducchi and coworkers recently showed TLR7 agonist-induced boosting of vaccine-induced antiviral immune responses in SIV-infected, cART-suppressed macaques that received therapeutic Ad26/MVA-vectored vaccination (57). In addition, although antiviral immunity was not formally evaluated, the apparent reductions in viral reservoirs in the TLR7 agonist-treated animals reported by Lim and colleagues (39) are suggestive of possible enhancement of antiviral immune responses in TLR7 agonist-treated animals. To determine if GS-9620 enhanced antiviral immune responses in our animals, we evaluated CD8⁺ T cell responses to SIV Gag and accessory gene (Nef, Rev, Tat, Vif, Vpr, and Vpx) peptide pools by ex vivo intracellular cytokine staining assays. CD8⁺ T cells collected prior to infection, prior to cART initiation (13 dpi), prior to GS-9620 dose 1.1 (75 weeks after infection), after dose 1.9, and after dose 1.12 were evaluated. For each of the cytokines measured, responses to both Gag and accessory gene products were negligible at each of these time points after infection and were indistinguishable from background responses measured for cells collected prior to infection (Figure 9A and Supplemental Figure 7). These results suggested that GS-9620 administration did not enhance antiviral CD8 responses while the animals were on cART.

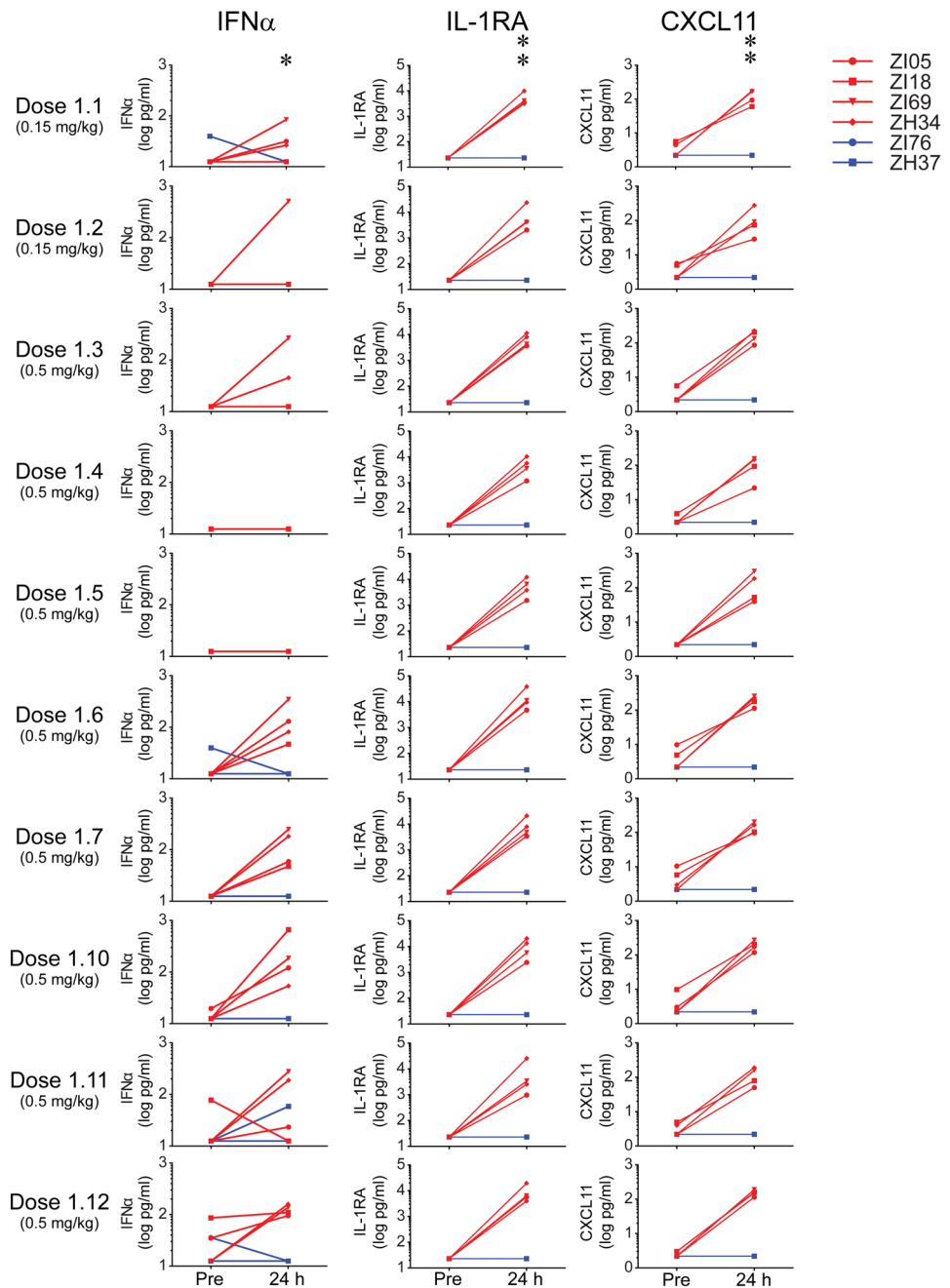


Figure 4. Increased plasma cytokine concentrations following GS-9620 administration. Shown are the concentrations in plasma prior to (Pre) and at 24 hours following the indicated doses of GS-9620 for 3 cytokines that were upregulated following GS-9620 administrations. Across the samples collected immediately prior to each dose, there were no significant differences between the GS-9620-treated animals (red plots) and the control animals (blue plots). Across the samples collected at 24 hours after each dose, plasma concentrations of all 3 cytokines were significantly higher in the GS-9620-treated animals than in the vehicle controls. * $P < 0.015$; ** $P < 0.001$.

Because the study animals were initiated on antiretroviral therapy early after infection (day 13) and maintained on cART for a long duration (75 weeks) prior to the first GS-9620 administration, antiviral CD8 responses may not have had adequate time to develop to sufficient levels or been exposed to sufficient viral antigen to be maintained during extended cART at sufficient levels to be measurably boosted when GS-9620 dosing was initiated. To test this hypothesis, animals were first maintained on cART for another 40 to 41 weeks following GS-9620 dose 1.12, at which point they initiated a second round of GS-9620 dosing comprising five 0.15-mg/kg doses administered once every 2 weeks (doses 2.1–2.5). Antiretroviral therapy was discontinued concomitant

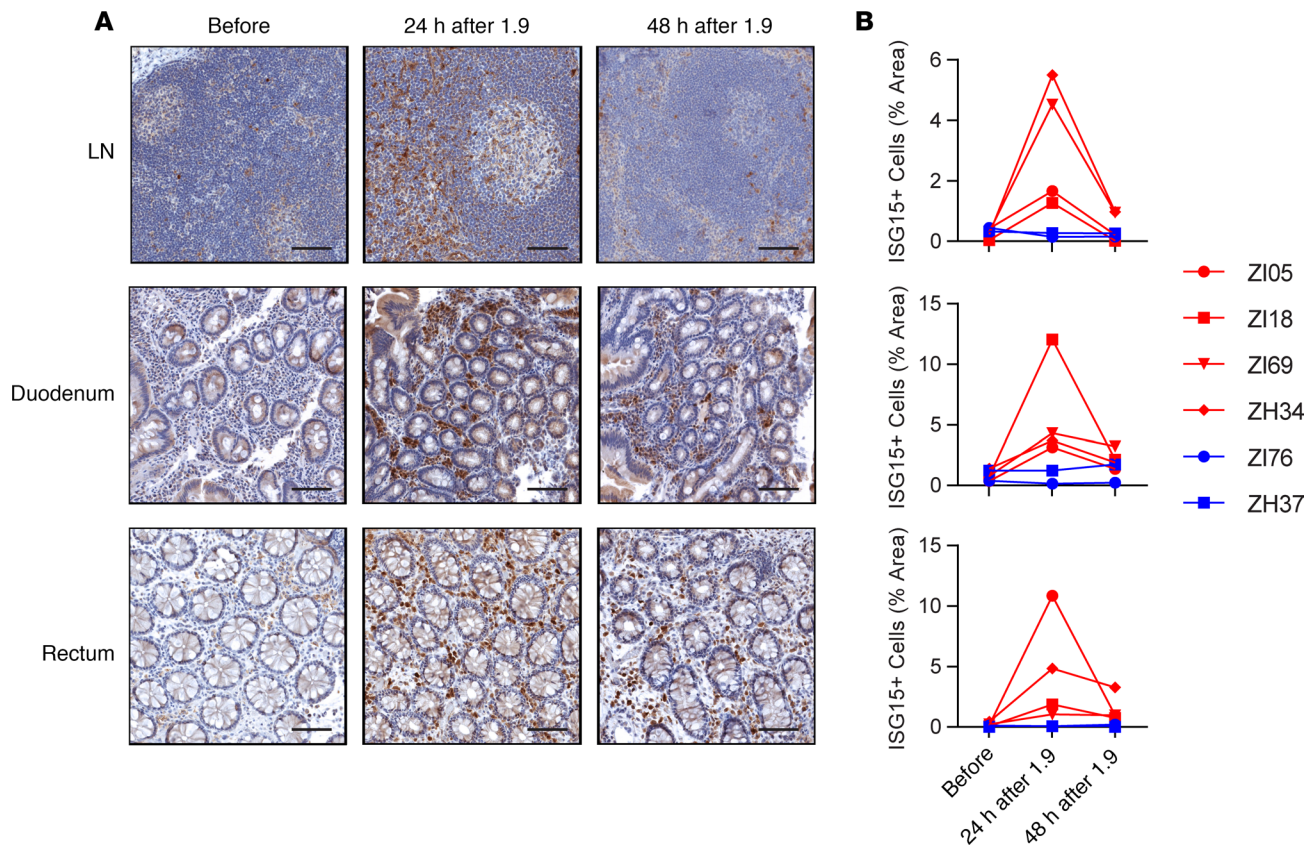


Figure 5. Increased expression of ISG15 protein in LNs and intestinal tissue following GS-9620 administration. (A) Representative images of ISG15 protein staining (brown) in LN, duodenal, and rectal tissue prior to the first dose of GS-9620 (Before) and at 24 hours and 48 hours following dose 1.9 for a GS-9620-treated animal. Images shown are from an intermediate responder, animal ZI69. Scale bars: 200 μ m. (B) Quantitative image analysis of ISG15 staining in LN (top), duodenal (middle), and rectal (bottom) tissue for all 6 study animals prior to the first dose of GS-9620 (Before) and at 24 hours and 48 hours following dose 1.9 for GS-9620-treated animals (red plots) and vehicle control animals (blue plots).

with the third dose (dose 2.3) to allow virologic rebound and the production of viral antigen to stimulate the generation of measurable antiviral immune responses. PBMC samples were studied by intracellular cytokine staining. For each of the cytokines evaluated, there were no differences between the GS-9620-treated and control groups across all of the time points sampled before cART release. In contrast, IFN- γ , TNF- α , and CD107a CD8⁺ T cell responses to viral accessory genes products were significantly elevated in the GS-9620 animals compared with the control animals during the off-cART phase of the study (Figure 9A), though this was not the case for responses to Gag (Supplemental Figure 7). Consistent with the difference being driven by immune responses being boosted within the GS-9620-treated animals, the IFN- γ , TNF- α , and CD107a CD8⁺ T cell responses to viral accessory genes products within the GS-9620-treated animals were significantly higher during the off-cART phase of the study compared with prior study time points within the same animals, while there were no differences in the antiviral immune responses in the control animals prior to and following cART release.

Viral rebound. No pVL blips were measured within the 36 weeks preceding cART discontinuation, including within the first 48 hours following any of doses 2.1 to 2.3, which were administered while the animals were still on cART or concomitantly with the final dose of cART. Antiretroviral therapy was discontinued after 144 weeks of treatment. Despite early cART initiation with prolonged treatment, pVLs rebounded to quantifiable levels in all 6 animals within 4 weeks of cART withdrawal (Figure 9B). During the first 4 weeks of off-cART viremia, peak rebound viral loads ranged from 2.6×10^3 to 6.2×10^6 vRNA copies/ml plasma. Thereafter, pVLs in 4 of 6 animals were largely maintained below 10^4 vRNA copies/ml for 24 weeks of follow-up, while they exceeded 10^6 vRNA copies/ml in the remaining 2 animals. Although antiviral CD8⁺ T cell responses were higher in the GS-9620-treated animals (Figure 9A), there was no evidence of enhanced virologic control in these animals (Figure 9B). Two of four GS-9620-treated animals and two of two vehicle control-treated animals demonstrated reduced off-cART viral loads, while the remaining two GS-9620-treated animals had elevated viral loads. Vehicle control animal ZH37 had

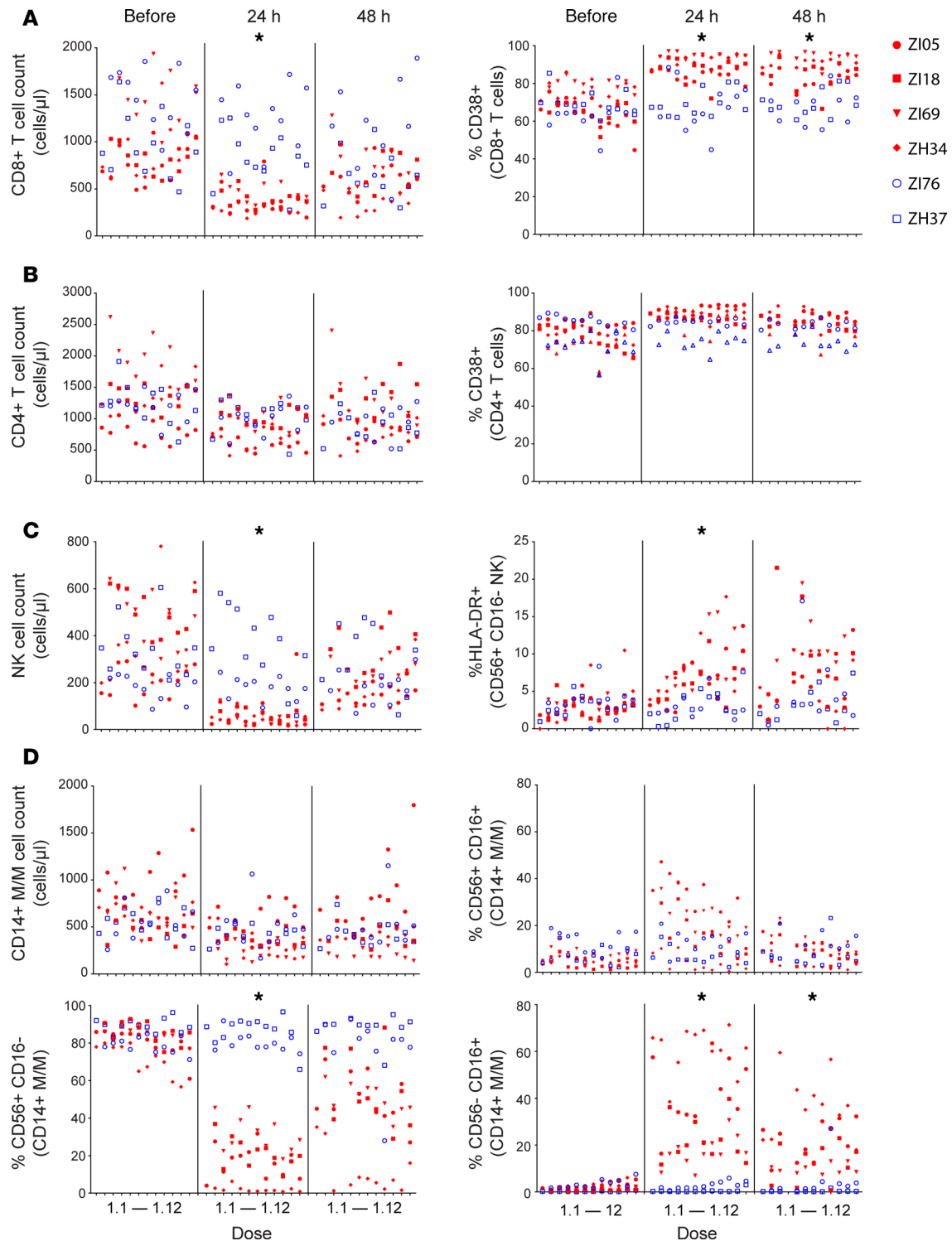


Figure 6. Immune cell populations respond to GS-9620 administration. Absolute cell counts and the frequency of cells expressing the indicated cell surface markers in blood immediately prior to (Before) and at 24 hours and 48 hours following each of the 12 doses of the first course of GS-9620 (doses 1.1 through 1.12) are shown for CD8⁺ T cells (A), CD4⁺ T cells (B), NK cells (C), and monocyte/macrophage (M/M) cell populations (D). For A–D, GS-9620-treated animals are shown with red plot symbols and vehicle control animals are shown with blue plot symbols. Significant differences between GS-9620-treated and control animals across the 24-hour and/or 48-hour time points for individual measurements are indicated with an asterisk ($P < 0.02$). There were no significant differences between the groups for any of the measures across the pretreatment time points or any measurements/time points not indicated with an asterisk. At 24 hours, there was a trend toward elevated CD38⁺CD4⁺ T cell percentage in the GS-9620 treatment group ($P = 0.073$).

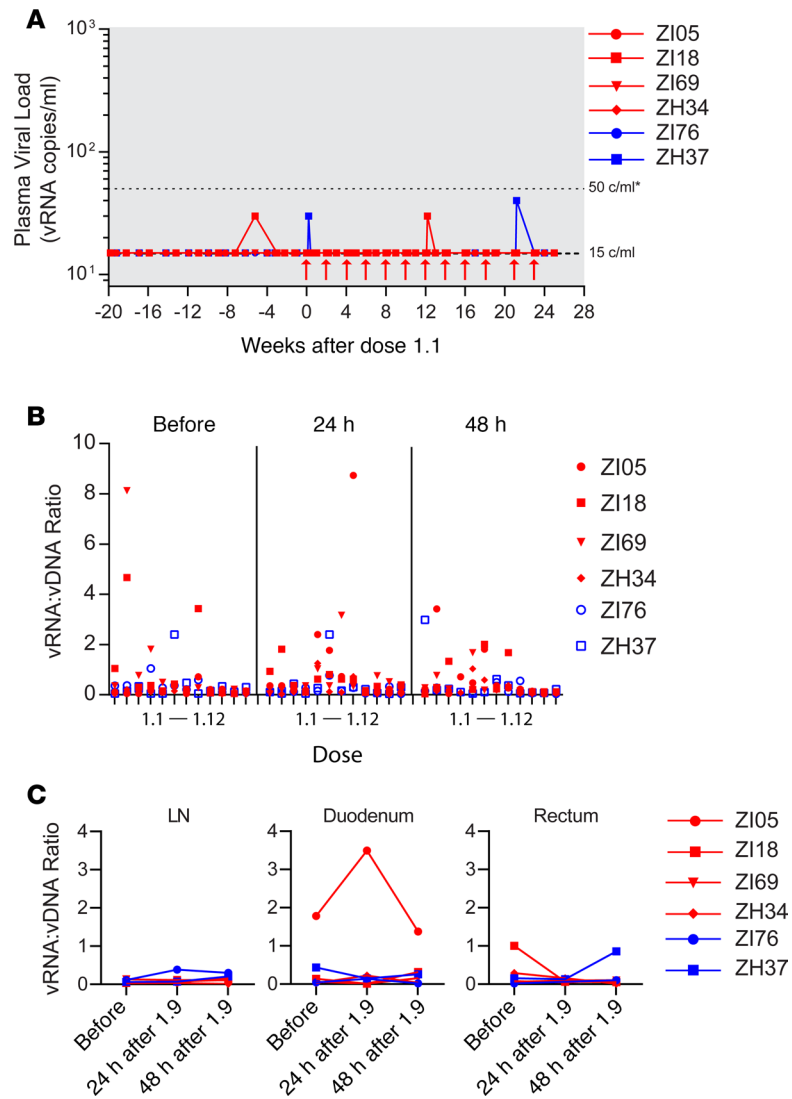


Figure 7. No evidence of increased viral expression following repeated GS-9620 administration. (A) Plasma viral loads prior to and during the first course of GS-9620 administration (doses 1.1 to 1.12). Red arrows indicate GS-9620 administrations at 0.15 mg/kg for the first two doses (1.1 and 1.2) and at 0.5 mg/kg for the last 10 doses (1.3 to 1.12). The 15-vRNA copy/ml threshold sensitivity of the viral load assay used is shown. Also shown for reference is the 50-vRNA copy/ml threshold sensitivity of the assay used in ref. 39. Dose 1.1 (time point 0) corresponds to 75 weeks after infection (wpi), or 73 weeks after cART initiation. (B and C) Cell/tissue-associated vRNA and vDNA content were quantified within the same samples by qRT-PCR and qPCR and the ratio of these values calculated. The calculated ratio in PBMC samples collected immediately prior to (Before) and at 24 hours and 48 hours following each of the 12 doses of the first course of GS-9620 (doses 1.1 through 1.12) are shown in B. The calculated ratio in LN, duodenal, and rectal tissue specimens collected and snap frozen prior to the first dose of GS-9620 (Before) and at 24 hours and 48 hours following dose 1.9 are shown in C. For A–C, GS-9620-treated animals are shown with red plot symbols and vehicle control animals are shown with blue plot symbols.

particularly blunted early off-cART viral replication kinetics, with viral loads maintained below 10^3 vRNA copies/ml for the first 10 weeks off cART. These results suggest that the timing of cART initiation and animal-specific host factors were primarily responsible for viremia levels after cART was withdrawn.

Discussion

Because of both their adjuvant-like potential to boost immune responses and their ability to induce the expression of HIV-1 in vitro and ex vivo, TLR7 agonists, such as GS-9620 and GS-986, have been viewed as particularly promising agents for HIV reservoir elimination (40, 58). Accordingly, GS-9620 is currently being evaluated in clinical trials for safety and residual virus elimination both in HIV-1–infected controllers (NCT03060447) and in those on suppressive cART (NCT02858401).

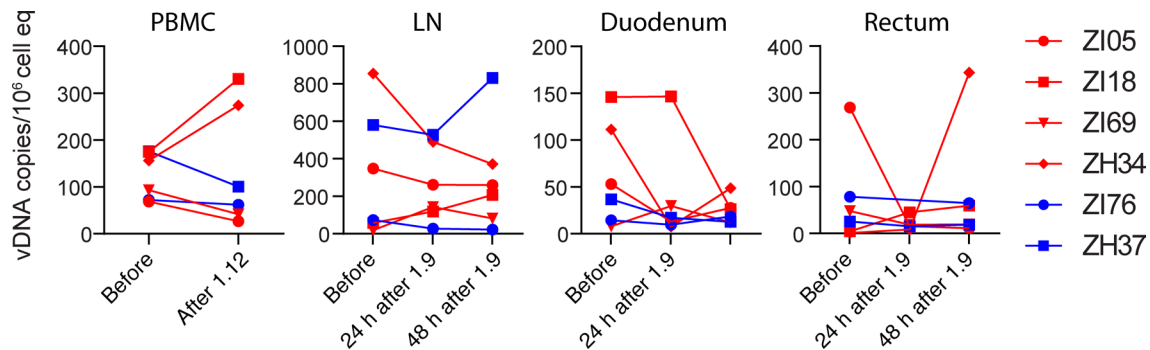


Figure 8. No changes in vDNA content associated with repeated GS-9620 administration. Shown are the vDNA levels in PBMCs prior to the first dose of GS-9620 and following dose 1.12 and in LN, duodenal, and rectal tissue collected and snap frozen prior to the first dose of GS-9620 and at 24 hours and 48 hours following dose 1.9. vDNA content was quantified by qPCR and normalized against the number of input cell equivalents (cell eq) analyzed, based on qPCR quantification of a host cellular gene in the same DNA extraction. GS-9620-treated animals are shown with red plot symbols and vehicle control animals are shown with blue plot symbols.

Three recent studies have reported on the administration of GS-9620 and/or GS-986 to SIV/SHIV-infected animals receiving suppressive cART, with apparently disparate findings regarding induction of virus expression (39, 57, 59). The first of these studies involved the administration of GS-986 or GS-9620 to SIVmac251-infected rhesus macaques started on cART 65 dpi and maintained on suppressive therapy for approximately 1 year before the initiation of TLR7 agonist dosing (39). Following several doses of TLR7 agonist that did not induce plasma vRNA blips, subsequent doses of GS-986/9620 were associated with transient plasma virus blips that reached levels between 500 and 1,000 vRNA copies/ml within 24–48 hours of dosing. While the biological mechanisms underlying the production of these virologic blips were not elucidated, the induction of elevated plasma viremia suggested latent viral genome reactivation and/or increased expression from cells already producing low amounts of virus (i.e., “active viral reservoirs”). Intriguingly, this study also demonstrated immunomodulatory effects of TLR7 agonist administration, including T cell activation, and reported reductions in vDNA levels and apparent virologic remission in a small subset of treated animals. Although antiviral immune responses were not formally evaluated, the data suggest that TLR7 agonist treatment resulted in the induction of virus production from a substantial fraction of cells harboring replication-competent genomes with concomitant boosting of existing antiviral immune responses or de novo generation of responses to enable the clearance of these virus-producing cells.

While two other studies by Borducchi and coworkers, one in SIVmac251-infected animals (57) and one in SHIV-SF162P3-infected animals (59), similarly reported T cell activation and other immunomodulatory effects of TLR7 agonist administration, plasma virus induction following TLR7 agonist dosing was not observed in either case. This apparent difference in the observed virologic response to TLR7 agonist treatment may have been due to differences in time to initiation of cART following virus infection, length of time on cART, and pVL assay sensitivities. In both of the Borducchi et al. studies, animals were started on suppressive cART very early after infection and during viral load ramp-up (7 dpi) and were monitored using a pVL assay with a higher reported threshold sensitivity (200 vRNA copies/ml) than that used by Lim et al. (39) (50 vRNA copies/ml). Under these study conditions, even if reactivated, the established viral reservoirs may have been too small to produce sufficient amounts of virus to be measured by the pVL assay used. Cell-associated vRNA levels, which may be a more sensitive measure of virus expression, were not evaluated in either early treatment study.

We designed our study to more carefully examine the virologic response to TLR7 agonist administration. Here, the study animals initiated suppressive therapy at 13 dpi, or approximately peak viremia, a time point intermediate to that used in prior studies and at which initial seeding of the viral reservoir is substantially complete (60). Antiretroviral therapy was then maintained for approximately 1.5 years before TLR7 agonist dosing. This timing and duration of cART were utilized to allow for the potential seeding of larger and more widely disseminated viral reservoirs than those established in the Borducchi et al. day 7 cART treatment studies (57, 59), while also ensuring that durable virologic suppression to <15 vRNA copies/ml had been established at the time of TLR7 agonist treatment. We additionally administered GS-9620 at a higher dose (0.5 mg/kg) than the highest dose of GS-9620 (0.15 mg/kg) or GS-986 (0.3 mg/kg) used in the prior studies.

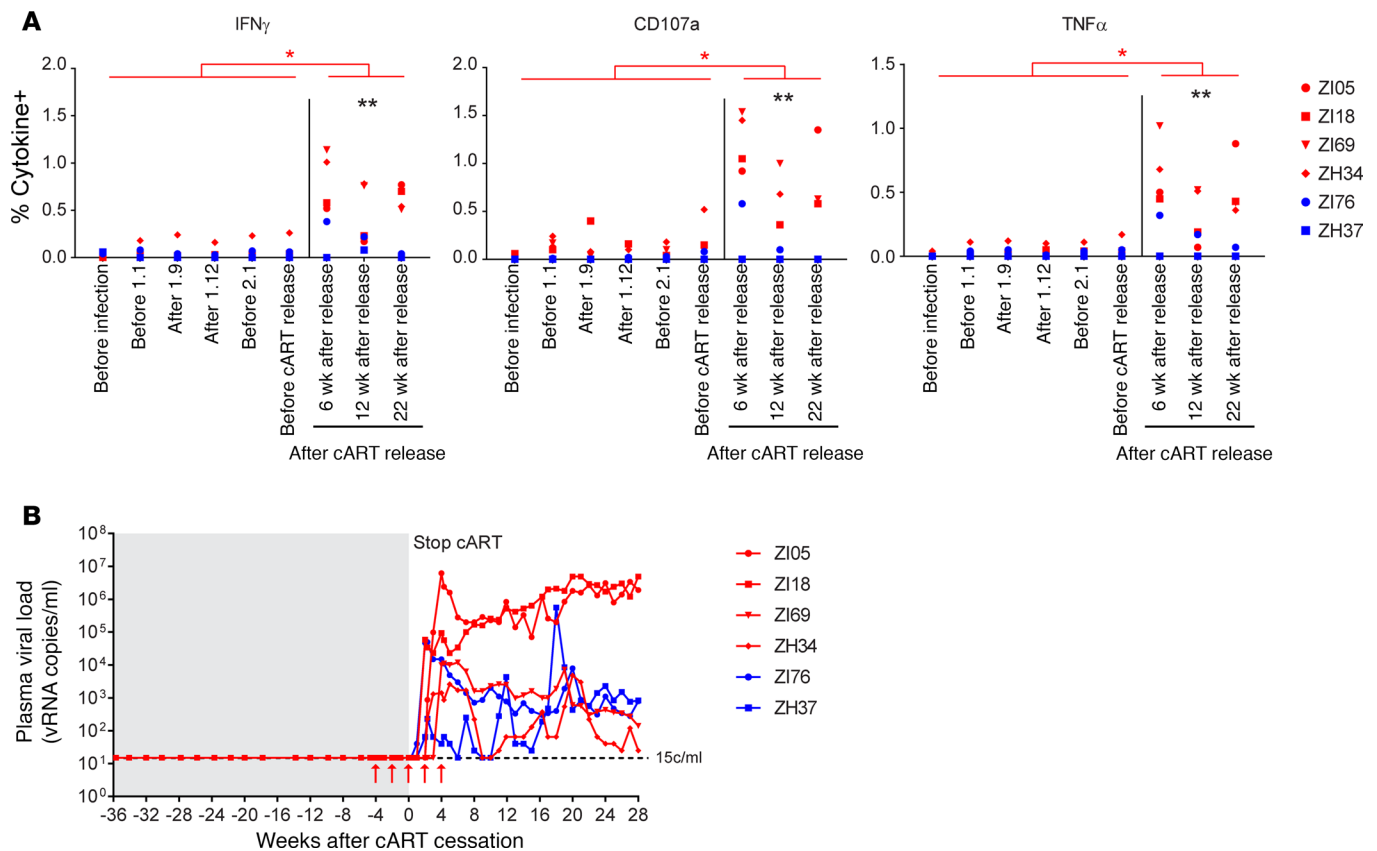


Figure 9. Immune response boosting with GS-9620 administration during off-cART viral rebound. (A) Intracellular staining of the indicated cytokines in CD8⁺ T cells collected at the indicated time points and stimulated with a peptide pool derived from SIV accessory genes. Within the GS-9620-treated animals, the frequency of stimulated cells expressing each of the 3 cytokines was significantly higher after cART release than before cART release ($*P < 0.01$). Within the control animals, the frequency of stimulated cells expressing each of the 3 cytokines prior to and after cART release was not significantly different. Prior to cART release, the frequency of stimulated cells expressing each cytokine was not significantly different between the GS-9620-treated and control animals, but after cART release, the frequency was significantly higher in GS-9620-treated animals compared with control animals ($**P < 0.03$). (B) Plasma viral loads prior to and following cART discontinuation. Red arrows indicate GS-9620 administrations at 0.15 mg/kg (doses 2.1 to 2.5). CART was discontinued after 144 weeks of treatment (time point 0). For A and B, GS-9620-treated animals are shown with red plots and vehicle control animals are shown with blue plots.

GS-9620 administration had clear immunomodulatory effects in our animals, confirming delivery of bioactive levels of drug. These changes were transient with relatively rapid kinetics, peaking within 24 hours and largely resolving by 48 hours to baseline levels. Multiple ISG mRNAs were significantly upregulated in PBMCs following GS-9620 administration. Among these ISGs, ISG15 expression increased the most dramatically, with RNA expression levels approximately 100-fold higher on average at 24 hours after dose than immediately prior to GS-9620 administration. Transient ISG15 upregulation following GS-9620 treatment was also identified at the protein level by immunohistochemical staining in key tissue sites of viral replication and reservoir establishment, such as LNs and upper and lower GI tract (48, 55), confirming drug activity in tissues as well as in the blood. Similar to results reported in the Lim and Borducchi studies (39, 57, 59), we also measured nonspecific activation of T cell and NK cell populations following TLR7 agonist administration. Intriguingly, we additionally saw significant transient declines in the absolute counts of CD8⁺ T cells and NK cells in blood 24 hours following GS-9620 dose. Most dramatic were the changes observed in circulating M/M populations following GS-9620 treatment. Within 24 hours of TLR7 agonist administration, we noted a striking decline in the frequency of M/M cells expressing CD56 with a concomitant, marked increase in CD16 (i.e., Fc γ RIII) expression. This intriguing upregulation in Fc γ RIII may suggest a possible mechanism for enhancement of antibody-mediated reservoir reduction (59). The plasma concentrations of several cytokines, including IFN- α , were also significantly upregulated following GS-9620 administration. These increases in plasma IFN- α concentration were likely due to the relatively high doses of GS-9620 used in this study (47, 61). Previous studies in humans and animal models have shown that reduced doses of GS-9620 can induce increases in the expression level of ISGs without mea-

surable systemic IFN induction (46, 47); such doses of GS-9620, which do not induce increases in systemic IFN- α , are likely to be more desirable for clinical application of GS-9620 than the elevated doses used here.

Despite clear evidence of robust pharmacodynamic activity of GS-9620 in our animals, including upregulation of the IFN- α and IFN pathways previously shown in *ex vivo* experiments to be required components of TLR7 agonist-mediated viral reactivation (40), frequent pVL monitoring using a highly sensitive pVL assay (quantification limit 15 vRNA copies/ml) did not reveal any increases in pVLs associated with GS-9620 administration. We also quantified cell- and tissue-associated vRNA and vDNA levels. In agreement with our pVL assay results, we did not measure any apparent increases in the vRNA/vDNA ratio, a presumptive measure of viral gene expression, in PBMCs, LNs, duodenum, or rectum.

Rare, non-GS-9620-associated pVL blips were readily detectable in our animals, as was cell-associated vRNA, suggesting that the established reservoir of infected cells in our animals was large enough to produce amounts of vRNA that would be detectable, if induced, using our assays. Moreover, the cell- and tissue-associated vDNA levels established in our animals were comparable to those reported in the animals that initiated cART during chronic infection in the Lim et al. study (39). Taken together, these findings suggest that robust virus induction by TLR7 agonists may be a function of the qualitative nature of the viral reservoirs present at the time of TLR7 agonist administration, which may in turn be a function of the timing and duration of suppressive therapy. We have found that the stable suppression of pVLs to levels below the detection limit of sensitive viral load assays in SIV-infected animals that initiate cART during the early chronic phase of infection may require a protracted duration of treatment (62–64). Thus, although the pVLs in the Lim et al. study animals were stably suppressed to <50 vRNA copies/ml, it is possible that the residual infected cell population in these animals comprised a significant proportion of so-called “active reservoirs” (i.e., those cells that are actively expressing viral gene products). This possibility is indirectly supported by the striking magnitude of virus induction identified by Lim et al., where pVLs increased by >10-fold following TLR7 agonist treatment (39). By contrast, the magnitude of virus induction in cultures of PBMCs from well-suppressed HIV-infected people treated *ex vivo* with GS-9620 were relatively modest (~2-fold) (40). Alternatively, the TLR7 agonist-induced virus expression reported by Lim et al. may reflect enhancement of or synergy with residual immune activation and inflammation processes that had not yet fully returned to baseline levels, given the timing and duration of cART. Further studies conducted in animals with varying start times after infection and durations of cART will be required to more clearly define the interplay between apparent TLR7 agonist-induced virus induction and the qualitative nature of the residual viral reservoir.

Although our study does not provide evidence to support a role for robust GS-9620-mediated induction of virus expression, we do provide additional evidence for GS-9620-mediated enhancement of antiviral immune responses, broadly consistent with the previously reported boosting of Ad26/MVA vaccine-induced immune responses (57). Although these elevated immune responses were not able to effect evident improvement in the degree of off-cART virologic control, our experiment was not optimally designed to test this question. Intriguingly, we did not observe immune response boosting during the first 12-dose course of GS-9620, perhaps due to the early initiation and prolonged duration of cART that preceded GS-9620 treatment and the associated negligible immune responses present in our animals. Although the Lim et al. study did not directly evaluate antiviral immune responses, the apparent decline in vDNA and viral remission reported for a subset of animals is suggestive of GS-9620-induced enhancement of preexisting potent immune responses capable of mediating reservoir reduction/clearance (39). We did not measure any declines in vDNA in blood or tissues associated with TLR7 agonist treatment, and plasma viremia rebounded in all 6 of our study animals within 4 weeks of cART discontinuation. This raises the possibility that a longer period of unsuppressed viral replication or therapeutic vaccination (57) may be required to develop an antiviral immune response that can be enhanced by TLR7 agonist treatment. Prolonged treatment with cART initiated at time points very early after infection may therefore have the paradoxical effect of limiting the size of the established viral reservoir while also limiting the potential effectiveness of therapies such as TLR7 agonists, because the “boost-able” immune response may be absent or too small to meaningfully enhance. However, a potential mechanism for complete clearance of all replication-competent viral genomes, including those that are truly latent and may not be reactivated by TLR7 agonist treatment, such as those established in our animals, remains unclear. Additional studies that further probe the relationship between response to TLR7 agonist treatment and the timing of cART initiation and duration, reservoir size, degree of virologic suppression as assessed using highly sensitive assays, and immune response development at the time of TLR7 agonist treatment will further our understanding of TLR7 agonist activity and its potential clinical utility.

Methods

Animals and treatment. Six male, purpose-bred, Indian-origin rhesus macaques (*Macaca mulatta*; ages 2.6–4.2 years at the time of initial virus infection) were housed at the NIH and cared for in accordance with American Association for the Accreditation of Laboratory Animal Care (AAALAC) standards in an AAALAC-accredited facility (Animal Welfare Assurance A4149-01). At the start of the study, all animals were free of cercopithecine herpesvirus 1, SIV, simian type-D retrovirus, and simian T lymphotropic virus type 1. Animal ZH34 possessed the Mamu-A*01 MHC class I allele, and animal ZI69 possessed the Mamu-B*08 MHC class I allele; the remaining animals were negative for Mamu-A*01, -B*08, and -B*17. Animals were intravenously inoculated with SIVmac239X (provided by Brandon Keele, Frederick National Laboratory) (41) and started on cART as previously described (42). At approximately 48 weeks after cART initiation, the dosage of FTC in the triple coformulation was reduced from 50 mg/kg to 40 mg/kg and was maintained at this level throughout the remainder of the cART treatment phase of the study. GS-9620 and vehicle control administrations were performed via oral gavage to sedated animals. GS-9620 treatment group animals received GS-9620 at 0.15 mg/ml/kg body weight (doses 1.1, 1.2, and 2.1 to 2.5) or at 0.5 mg/ml/kg body weight (doses 1.3 to 1.12), while vehicle control group animals instead received an equivalent volume of drug vehicle (0.005% propyl gallate in water). All animals received cART for 144 weeks. The final dose of cART was administered on the same day as GS-9620 (or vehicle control) dose 2.3. LN biopsies, duodenal pinch biopsies, and rectal pinch biopsies were collected 2 weeks prior to the first dose of GS-9620 (dose 1.1) and at 24 hours and 48 hours following dose 1.9.

Sample collection and preparation. Whole blood, LN biopsies, and duodenal and rectal pinch biopsies were collected from sedated animals. Endoscopic duodenal pinch biopsy specimens and rectal pinch biopsy specimens were obtained using biopsy forceps under endoscopic and direct visualization, respectively. Freshly collected LN, duodenal, and rectal tissue specimens were collected into tubes containing 4% paraformaldehyde or into empty tubes and snap frozen in liquid nitrogen and stored at -80°C . Plasma for vRNA quantification and cytokine concentration determinations and PBMCs for flow cytometric assays, functional intracellular cytokine staining assays, and cell-associated vRNA and vDNA quantification were prepared from blood collected in EDTA Vacutainer tubes (BD). Following separation from whole blood by centrifugation, plasma aliquots were stored at -80°C . PBMCs were isolated from whole blood by Ficoll-Paque Plus (GE Healthcare) gradient centrifugation. Portions of isolated PBMC samples were cryopreserved viably or as dry cell pellets.

pVLs. For the first 50 weeks of the study, quantification of SIV RNA in plasma was performed using a qRT-PCR assay with a threshold quantification limit of 30 vRNA copies/ml, as previously described (63). Thereafter, a qRT-PCR assay with a threshold quantification limit of 15 vRNA copies/ml was used, as previously described (65).

Cell-associated viral loads. Cell-associated vRNA and vDNA levels in PBMCs and biopsy tissues were analyzed essentially as described, using quantitative PCR and RT-PCR assays targeting a conserved sequence in gag (66, 67).

ISG expression. Relative ISG expression levels were determined by qRT-PCR-based expression array. Cell-associated RNA was extracted from thawed, previously cryopreserved PBMC pellets, each containing approximately 2 million cells, using the RNeasy Plus Mini Kit (Qiagen) according to the manufacturer's instructions. Extracted RNA was quantified by NanoDrop (Thermo Fisher) and quality checked by bioanalyzer using the RNA 6000 Nano kit (Agilent), according to the manufacturer's instructions. Extracted RNA (150 ng per sample) was next used to generate cDNA using the RT² First Strand Kit, with ISG sequences in the cDNA quantified by qPCR on an ABI 7500 real-time PCR system using the Rhesus Macaque Type I Interferon Response RT² Profiler PCR Array with the RT² SYBR Green ROX qPCR Mastermix (Qiagen), all according to the manufacturers' instructions. Fold regulation was calculated by the $\Delta\Delta C_T$ method using the RT² Profiler PCR Array Data Analysis webportal (<https://www.qiagen.com/us/shop/genes-and-pathways/data-analysis-center-overview-page>).

Flow cytometric assays. Antibodies and reagents were obtained from BD Biosciences, unless indicated otherwise, and data analysis was performed using FCS Express (De Novo Software). Antibody panel validation and population gating were performed using fluorescence-minus-one and corresponding biological controls. For absolute cell counting, 50 μl EDTA-anti-coagulated whole blood was incubated for 20 minutes with the antibody panels listed below. 2 ml of $1 \times$ 1-step Fix/Lyse Solution (eBioscience) was then added, incubated for 10 minutes, and then approximately 50,000 CD45⁺CD3⁺ gated cells were acquired per

sample on a BD FACSVerse flow cytometer equipped with a volumetric flow sensor. For panel 1, we used the following antibodies: CD20 Pacific Blue (2H7, BioLegend), CD28 Brilliant Violet (BV) 510 (CD28.2), CD45 FITC (DO58-1283), CD3 PE (SP34-2), CD95 PE-Cy5 (DX2), CD8 α PE-Cy7 (SK1), CD4 APC (L200), and CD14 APC-Cy7 (M5E2, BioLegend). For panel 2, we used the following antibodies: CD20 Pacific Blue, CD3 Pacific Blue (SP34-2), CD14 Pacific Blue (M5E2, BioLegend), CD123 BV510 (6H6, BioLegend), CD45 FITC, CD16 PE (3G8), CD56 PE-Cy5 (B159), CD8 α PE-Cy7, CD11c APC (3.9, BioLegend), and HLA-DR APC-Cy7 (L243, BioLegend). For immunophenotyping, 100 μ l EDTA-anti-coagulated whole blood or 1×10^6 freshly isolated tissue-suspension cells were incubated for 20 minutes using the following antibody panel: CD4 BV421 (OKT4, BioLegend), CD123 BV510, CD27 BV605 (O323, BioLegend), CD95 BV711 (DX2, BioLegend), CD16 BV785 (3G8, BioLegend), CD20 PerCP-Cy5.5 (2H7, BioLegend), CD14 APC (M5E2, BioLegend), HLA-DR Alexa Fluor 700 (L243, BioLegend), CD3 APC-Cy7 (SP34-2), CD38 PE (OK10; NIH Nonhuman Primate Reagent Resource), CD28 ECD (CD28.2, Beckman Coulter), CD56 PE-Cy5 and CD8 α PE-Cy7. Samples were lysed with $1 \times$ BD FACS Lyse buffer, washed, and then treated with BD Cytofix/Cytoperm buffer. Samples were incubated with an intracellular staining panel containing Ki67 FITC (B56) and CD69 BV650 (FN50, BioLegend) antibodies for 30 minutes, and approximately 200,000 CD3⁺ T cells were acquired for each sample using a BD LSR-II flow cytometer. To assess homing marker (CCR7 and CXCR5) expression, viably cryopreserved PBMC samples were quickly thawed at 37°C, washed, and incubated overnight at 37°C in RPMI 1640 supplemented with 10% fetal bovine serum, 1% penicillin/streptomycin, and 1% L-glutamine. Cells were then stained with CD3 APC Cy7 (SP34-2), CD4 Pacific Blue (OKT4, BioLegend), CD8 α PerCP Cy5.5 (SK1), CCR7 PE Cy7 (G043H7, BioLegend), CXCR5 APC (MU5UBEE, ebioscience) and Live/Dead fixable blue (Invitrogen) for 20 minutes and then fixed and acquired on a BD LSR Fortessa X-20.

Intracellular cytokine staining. Antibodies were obtained from BD Biosciences unless otherwise indicated. 10^6 quickly thawed, cryopreserved PBMCs were stimulated for 8 hours at 37°C with a pool of 2 μ g/ml overlapping 15mer SIVmac239 accessory (nef, rev, tat, vif, vpr, and vpx) or gag peptides (AIDS Reagent Program, Division of AIDS, NIAID, NIH) in the presence of CD107a BV785 antibody (H4A3, BioLegend). Phorbol 12-myristate 13-acetate with Ionomycin (MilliporeSigma) or DMSO were used as positive and negative controls, respectively, and brefeldin A (MilliporeSigma) mixed with GolgiStop (BD) was added after 1 hour to block protein transport. Immediately following the 8 hours incubation, samples were placed at 4°C until staining. Samples were surface stained with Yellow Fluorescent Reactive Dye (to exclude dead cells, Invitrogen), CD4 Pacific Blue (OKT4, BioLegend), CD28 ECD, CD95 PE-Cy5, and CD8 α PE-Cy7; lysed; fixed; and permeabilized as described above and then incubated with CD3 APC-Cy7, IFN- α FITC (B27), MIP-1 β PE (D21-1351), TNF- α BV711 (MAb11, BioLegend), and IL-2 APC (MQ1-17H12). Approximately 200,000 live CD3⁺ T cells were acquired for each sample using an HTS-equipped BD LSR-II cytometer.

Plasma cytokine measurements. Thawed plasmas were analyzed for cytokine/chemokine levels by custom primate 8-plex (Bio-Plex Multiplex Immunoassay, Bio-Rad) per manufacturer's instructions, which included measurements for the following cytokines and chemokines: IL-1RA, IL-6, IL-8 (CXCL8), CXCL11, MCP-1 (CCL2), RANTES (CCL5), TNF- α , and sCD40L. IFN- α plasma levels were determined by cynomolgus/rhesus specific ELISA per manufacturer's instructions (PBL Assay Science).

Tissue staining. ISG15 (rabbit anti-ISG15, HPA004627; Sigma-Aldrich) immunohistochemical staining was performed on formalin-fixed, paraffin-embedded LN, duodenal, and rectal tissues sections of 5 μ m as previously described (68). All slides were scanned at high magnification ($\times 200$) using the ScanScope CS or AT2 System (Aperio Technologies). Regions of interest (500 \times 500 μ m) were identified and high-resolution images were extracted from these whole-tissue scans. The percentage area of ISG15-positive staining was quantified using Photoshop CS5, Noiseware 5 (Imagenomic) for noise reduction, and Fovea Pro beta 5 (Reindeer Graphics) image analysis tools.

Statistics. Data in this study were analyzed with longitudinal repeated-measures ANOVA (69), linear mixed-effects models (70), and regression analysis. Immune cell subset (CD8⁺, CD4⁺, NK, etc.) data for 4 GS-9620-treated and 2 vehicle control animals were recorded for varying numbers of occasions, within multiple treatment phases. Repeated-measures analyses (in which the "repeated" measurements are recorded for the same animal on more than one occasion) and mixed-effects models take into consideration the correlation/covariation of responses within the same animal over time. Mixed-effects models were used to compare GS-9620-treated and vehicle control groups, adjusting for within-animal covariation and also correcting for heterogeneity between groups. Assumptions for homogeneity of variance/covariance between

GS-9620-treated and vehicle control animals were routinely tested and satisfied. For analyses of shifts in phases, factors in the experimental setup — animals, occasions, phases, occasions within phases, etc., — were partitioned into orthogonal components. Expected values of the factor mean squares were computed and correct variance ratios were calculated to test for questions of interest, in particular, for differences among phases across time (69). *P* values of less than 0.05 were considered significant.

Study approval. All work involving research animals was conducted under a protocol approved by the Institutional Animal Care and Use Committee of the National Cancer Institute (protocol AVP-035) and adhered to the standards of the *Guide for the Care and Use of Laboratory Animals* (National Research Council, 2011) in accordance with the Animal Welfare Act.

Author contributions

GQD, JH, RG, and JDL designed the study. GQD, YL, CD, MN, KO, JAT, CP, WJB, VC, AW, RW, BB, MH, EC, LS, RF, JK, RK, MWB, CMT, JDE, TLB, JH, and JDL conducted the experiments. GQD, YL, CD, KO, JAT, CP, WJB, BB, MH, EC, LS, RF, CMT, JDE, TLB, and JH acquired the data. GQD, WGA, YL, CD, TM, CMT, JDE, JH, and JDL analyzed the data. GQD, JH, RG, and JDL wrote the manuscript.

Acknowledgments

The authors thank the animal husbandry and technical staff of the Laboratory Animal Sciences Program, Frederick National Laboratory for Cancer Research, for expert animal care and handling. This work was supported by federal funds from the National Cancer Institute, NIH (contract HHSN261200800001E). The content of this publication does not necessarily reflect the views or policies of the Department of Health and Human Services, nor does mention of trade names, commercial products, or organizations imply endorsement by the US government.

Address correspondence to: Jeffrey D. Lifson, PO Box B, Frederick, Maryland 21702, USA. Phone: 1.301.846.1408; Email: jeffrey.lifson@nih.gov.

JDE's present address is: Vaccine and Gene Therapy Institute and Oregon National Primate Research Center, Oregon Health and Science University, Beaverton, Oregon, USA.

- Davey RT, et al. HIV-1 and T cell dynamics after interruption of highly active antiretroviral therapy (HAART) in patients with a history of sustained viral suppression. *Proc Natl Acad Sci USA*. 1999;96(26):15109–15114.
- Chun TW, et al. Rebound of plasma viremia following cessation of antiretroviral therapy despite profoundly low levels of HIV reservoir: implications for eradication. *AIDS*. 2010;24(18):2803–2808.
- Antiretroviral Therapy Cohort Collaboration. Survival of HIV-positive patients starting antiretroviral therapy between 1996 and 2013: a collaborative analysis of cohort studies. *Lancet HIV*. 2017;4(8):e349–e356.
- Cleary S, McIntyre D. Financing equitable access to antiretroviral treatment in South Africa. *BMC Health Serv Res*. 2010;10 Suppl 1:S2.
- Al-Dakkak I, Patel S, McCann E, Gadkari A, Prajapati G, Maiese EM. The impact of specific HIV treatment-related adverse events on adherence to antiretroviral therapy: a systematic review and meta-analysis. *AIDS Care*. 2013;25(4):400–414.
- Hunt PW, Lee SA, Siedner MJ. Immunologic Biomarkers, Morbidity, and Mortality in Treated HIV Infection. *J Infect Dis*. 2016;214 Suppl 2:S44–S50.
- Buzón MJ, et al. HIV-1 replication and immune dynamics are affected by raltegravir intensification of HAART-suppressed subjects. *Nat Med*. 2010;16(4):460–465.
- Llibre JM, et al. Treatment intensification with raltegravir in subjects with sustained HIV-1 viraemia suppression: a randomized 48-week study. *Antivir Ther (Lond)*. 2012;17(2):355–364.
- Yukl SA, et al. Effect of raltegravir-containing intensification on HIV burden and T-cell activation in multiple gut sites of HIV-positive adults on suppressive antiretroviral therapy. *AIDS*. 2010;24(16):2451–2460.
- Jain V, et al. Antiretroviral therapy initiated within 6 months of HIV infection is associated with lower T-cell activation and smaller HIV reservoir size. *J Infect Dis*. 2013;208(8):1202–1211.
- Chun TW, Finzi D, Margolick J, Chadwick K, Schwartz D, Siliciano RF. In vivo fate of HIV-1-infected T cells: quantitative analysis of the transition to stable latency. *Nat Med*. 1995;1(12):1284–1290.
- Chun TW, et al. Quantification of latent tissue reservoirs and total body viral load in HIV-1 infection. *Nature*. 1997;387(6629):183–188.
- Finzi D, et al. Latent infection of CD4+ T cells provides a mechanism for lifelong persistence of HIV-1, even in patients on effective combination therapy. *Nat Med*. 1999;5(5):512–517.
- Wong JK, et al. Recovery of replication-competent HIV despite prolonged suppression of plasma viremia. *Science*. 1997;278(5341):1291–1295.
- Siliciano JD, et al. Long-term follow-up studies confirm the stability of the latent reservoir for HIV-1 in resting CD4+ T cells.

- Nat Med.* 2003;9(6):727–728.
18. Maldarelli F, et al. HIV latency. Specific HIV integration sites are linked to clonal expansion and persistence of infected cells. *Science.* 2014;345(6193):179–183.
 19. Wagner TA, et al. HIV latency. Proliferation of cells with HIV integrated into cancer genes contributes to persistent infection. *Science.* 2014;345(6196):570–573.
 20. Cohn LB, et al. HIV-1 integration landscape during latent and active infection. *Cell.* 2015;160(3):420–432.
 21. Kearney MF, et al. Origin of Rebound Plasma HIV Includes Cells with Identical Proviruses That Are Transcriptionally Active before Stopping of Antiretroviral Therapy. *J Virol.* 2016;90(3):1369–1376.
 22. Simonetti FR, et al. Clonally expanded CD4+ T cells can produce infectious HIV-1 in vivo. *Proc Natl Acad Sci USA.* 2016;113(7):1883–1888.
 23. Fletcher CV, et al. Persistent HIV-1 replication is associated with lower antiretroviral drug concentrations in lymphatic tissues. *Proc Natl Acad Sci USA.* 2014;111(6):2307–2312.
 24. Lorenzo-Redondo R, et al. Persistent HIV-1 replication maintains the tissue reservoir during therapy. *Nature.* 2016;530(7588):51–56.
 25. Hatano H, et al. Increase in 2-long terminal repeat circles and decrease in D-dimer after raltegravir intensification in patients with treated HIV infection: a randomized, placebo-controlled trial. *J Infect Dis.* 2013;208(9):1436–1442.
 26. Sigal A, et al. Cell-to-cell spread of HIV permits ongoing replication despite antiretroviral therapy. *Nature.* 2011;477(7362):95–98.
 27. Kearney MF, et al. Lack of detectable HIV-1 molecular evolution during suppressive antiretroviral therapy. *PLoS Pathog.* 2014;10(3):e1004010.
 28. Kearney MF, et al. Ongoing HIV Replication During ART Reconsidered. *Open Forum Infect Dis.* 2017;4(3):ofx173.
 29. Joos B, et al. HIV rebounds from latently infected cells, rather than from continuing low-level replication. *Proc Natl Acad Sci USA.* 2008;105(43):16725–16730.
 30. Josefsson L, et al. The HIV-1 reservoir in eight patients on long-term suppressive antiretroviral therapy is stable with few genetic changes over time. *Proc Natl Acad Sci USA.* 2013;110(51):E4987–E4996.
 31. Evering TH, et al. Absence of HIV-1 evolution in the gut-associated lymphoid tissue from patients on combination antiviral therapy initiated during primary infection. *PLoS Pathog.* 2012;8(2):e1002506.
 32. McMahon D, et al. Short-course raltegravir intensification does not reduce persistent low-level viremia in patients with HIV-1 suppression during receipt of combination antiretroviral therapy. *Clin Infect Dis.* 2010;50(6):912–919.
 33. Hatano H, et al. A randomized, controlled trial of raltegravir intensification in antiretroviral-treated, HIV-infected patients with a suboptimal CD4+ T cell response. *J Infect Dis.* 2011;203(7):960–968.
 34. Gandhi RT, et al. No effect of raltegravir intensification on viral replication markers in the blood of HIV-1-infected patients receiving antiretroviral therapy. *J Acquir Immune Defic Syndr.* 2012;59(3):229–235.
 35. Vallejo A, et al. The effect of intensification with raltegravir on the HIV-1 reservoir of latently infected memory CD4 T cells in suppressed patients. *AIDS.* 2012;26(15):1885–1894.
 36. Dinoso JB, et al. Treatment intensification does not reduce residual HIV-1 viremia in patients on highly active antiretroviral therapy. *Proc Natl Acad Sci USA.* 2009;106(23):9403–9408.
 37. Mombelli M, et al. Histone deacetylase inhibitors impair antibacterial defenses of macrophages. *J Infect Dis.* 2011;204(9):1367–1374.
 38. Alvarez-Breckenridge CA, et al. The histone deacetylase inhibitor valproic acid lessens NK cell action against oncolytic virus-infected glioblastoma cells by inhibition of STAT5/T-BET signaling and generation of gamma interferon. *J Virol.* 2012;86(8):4566–4577.
 39. Kelly-Sell MJ, et al. The histone deacetylase inhibitor, romidepsin, suppresses cellular immune functions of cutaneous T-cell lymphoma patients. *Am J Hematol.* 2012;87(4):354–360.
 40. Jones RB, et al. Histone deacetylase inhibitors impair the elimination of HIV-infected cells by cytotoxic T-lymphocytes. *PLoS Pathog.* 2014;10(8):e1004287.
 41. Lim SY, et al. TLR7 agonists induce transient viremia and reduce the viral reservoir in SIV-infected rhesus macaques on antiretroviral therapy. *Sci Transl Med.* 2018;10(439):eaa04521.
 42. Tsai A, et al. Toll-Like Receptor 7 Agonist GS-9620 Induces HIV Expression and HIV-Specific Immunity in Cells from HIV-Infected Individuals on Suppressive Antiretroviral Therapy. *J Virol.* 2017;91(8):e02166-16.
 43. Del Prete GQ, et al. Molecularly tagged simian immunodeficiency virus SIVmac239 synthetic swarm for tracking independent infection events. *J Virol.* 2014;88(14):8077–8090.
 44. Del Prete GQ, et al. Short Communication: Comparative Evaluation of Coformulated Injectable Combination Antiretroviral Therapy Regimens in Simian Immunodeficiency Virus-Infected Rhesus Macaques. *AIDS Res Hum Retroviruses.* 2016;32(2):163–168.
 45. Vasilakos JP, Tomai MA. The use of Toll-like receptor 7/8 agonists as vaccine adjuvants. *Expert Rev Vaccines.* 2013;12(7):809–819.
 46. Lanford RE, et al. GS-9620, an oral agonist of Toll-like receptor-7, induces prolonged suppression of hepatitis B virus in chronically infected chimpanzees. *Gastroenterology.* 2013;144(7):1508–1517.
 47. Lopatin U, et al. Safety, pharmacokinetics and pharmacodynamics of GS-9620, an oral Toll-like receptor 7 agonist. *Antivir Ther.* 2013;18(3):409–418.
 48. Janssen HLA, et al. Safety, efficacy and pharmacodynamics of vesatolimod (GS-9620) in virally suppressed patients with chronic hepatitis B. *J Hepatol.* 2018;68(3):431–440.
 49. Fosdick A, et al. Pharmacokinetic and pharmacodynamic properties of GS-9620, a novel Toll-like receptor 7 agonist, demonstrate interferon-stimulated gene induction without detectable serum interferon at low oral doses. *J Pharmacol Exp Ther.* 2014;348(1):96–105.
 50. Estes JD, et al. Defining total-body AIDS-virus burden with implications for curative strategies. *Nat Med.* 2017;23(11):1271–1276.
 51. Folkvord JM, Armon C, Connick E. Lymphoid follicles are sites of heightened human immunodeficiency virus type 1 (HIV-1) replication and reduced antiretroviral effector mechanisms. *AIDS Res Hum Retroviruses.* 2005;21(5):363–370.
 52. Connick E, et al. CTL fail to accumulate at sites of HIV-1 replication in lymphoid tissue. *J Immunol.* 2007;178(11):6975–6983.
 53. Brenchley JM, et al. Differential infection patterns of CD4+ T cells and lymphoid tissue viral burden distinguish progressive and nonprogressive lentiviral infections. *Blood.* 2012;120(20):4172–4181.

52. Perreau M, et al. Follicular helper T cells serve as the major CD4 T cell compartment for HIV-1 infection, replication, and production. *J Exp Med*. 2013;210(1):143–156.
53. Fukazawa Y, et al. B cell follicle sanctuary permits persistent productive simian immunodeficiency virus infection in elite controllers. *Nat Med*. 2015;21(2):132–139.
54. Banga R, et al. PD-1(+) and follicular helper T cells are responsible for persistent HIV-1 transcription in treated aviremic individuals. *Nat Med*. 2016;22(7):754–761.
55. Deleage C, et al. Defining HIV and SIV Reservoirs in Lymphoid Tissues. *Pathog Immun*. 2016;1(1):68–106.
56. Carter DL, et al. CD56 identifies monocytes and not natural killer cells in rhesus macaques. *Cytometry*. 1999;37(1):41–50.
57. Borducchi EN, et al. Ad26/MVA therapeutic vaccination with TLR7 stimulation in SIV-infected rhesus monkeys. *Nature*. 2016;540(7632):284–287.
58. Macedo AB, et al. Dual TLR2 and TLR7 agonists as HIV latency-reversing agents. *JCI Insight*. 2018;3(19):e122673.
59. Borducchi EN, et al. Antibody and TLR7 agonist delay viral rebound in SHIV-infected monkeys. *Nature*. 2018;563(7731):360–364.
60. Okoye AA, et al. Early antiretroviral therapy limits SIV reservoir establishment to delay or prevent post-treatment viral rebound. *Nat Med*. 2018;24(9):1430–1440.
61. Whitney JB, et al. Rapid seeding of the viral reservoir prior to SIV viraemia in rhesus monkeys. *Nature*. 2014;512(7512):74–77.
62. Del Prete GQ, Lifson JD. Considerations in the development of nonhuman primate models of combination antiretroviral therapy for studies of AIDS virus suppression, residual virus, and curative strategies. *Curr Opin HIV AIDS*. 2013;8(4):262–272.
63. Del Prete GQ, et al. Effect of suberoylanilide hydroxamic acid (SAHA) administration on the residual virus pool in a model of combination antiretroviral therapy-mediated suppression in SIVmac239-infected indian rhesus macaques. *Antimicrob Agents Chemother*. 2014;58(11):6790–6806.
64. Del Prete GQ, et al. Elevated Plasma Viral Loads in Romidepsin-Treated Simian Immunodeficiency Virus-Infected Rhesus Macaques on Suppressive Combination Antiretroviral Therapy. *Antimicrob Agents Chemother*. 2015;60(3):1560–1572.
65. Li H, et al. Envelope residue 375 substitutions in simian-human immunodeficiency viruses enhance CD4 binding and replication in rhesus macaques. *Proc Natl Acad Sci USA*. 2016;113(24):E3413–E3422.
66. Hansen SG, et al. Immune clearance of highly pathogenic SIV infection. *Nature*. 2013;502(7469):100–104.
67. Hansen SG, et al. Addendum: Immune clearance of highly pathogenic SIV infection. *Nature*. 2017;547(7661):123–124.
68. Deleage C, et al. Impact of early cART in the gut during acute HIV infection. *JCI Insight*. 2016;1(10):e87065.
69. Crowder MJ, and Hand DJ. *Analysis of Repeated Measures*. London: Chapman and Hall; 1990:27–42.
70. Pinheiro JC, Bates DM. *Mixed-Effects Models in S and S-PLUS*. New York: Springer-Verlag; 2000. *New York: Springer-Verlag; 2000.*